



## Cultivation reduces quantities of mineral-organic associations in the form of amorphous coprecipitates

Floriane Jamoteau<sup>1,2,3,4\*</sup>, Emmanuel Doelsch<sup>2,3</sup>, Nithavong Cam<sup>1</sup>, Clément Levard<sup>1</sup>, Thierry Woignier<sup>5,6</sup>,  
Adrien Boulineau<sup>7</sup>, Francois Saint-Antonin<sup>7</sup>, Sufal Swaraj<sup>8</sup>, Ghislain Gassier<sup>1</sup>, Adrien Duvivier<sup>1</sup>, Daniel  
5 Borschneck<sup>1</sup>, Marie-Laure Pons<sup>1</sup>, Perrine Chaurand<sup>1</sup>, Vladimir Vidal<sup>1</sup>, Nicolas Brouilly<sup>9</sup>, Isabelle Basile-  
Doelsch<sup>1</sup>

<sup>1</sup>Aix Marseille Université, CNRS, IRD, INRAE, Coll France, CEREGE, Aix-en-Provence, 13545, France

<sup>2</sup>CIRAD, UPR Recyclage et risque, Montpellier, F-34398, France

<sup>3</sup>Recyclage et Risque, Univ Montpellier, CIRAD, Montpellier, F-34398, France

10 <sup>4</sup>Institute of Earth Surface Dynamics, University of Lausanne, Lausanne, 1015, Switzerland

<sup>5</sup>Campus Agro Environnemental Caraïbes-IMBE-CNRS, B.P. 214, Petit Morne, Le Lamentin, Martinique, 97232, France

<sup>6</sup>Laboratoire Charles Coulomb UMR 5221 CNRS-UM2, Université Montpellier 2, Montpellier Cedex5, 34095, France

<sup>7</sup>Université Grenoble Alpes, CEA, LITEN, Grenoble, 38100, France

<sup>8</sup>Synchrotron SOLEIL, L'Orme des Merisiers, Departementale 128, Saint-Aubin, 91190, France

15 <sup>9</sup>Aix-Marseille Université, CNRS UMR 7288, IBDM, Marseille, 13000, France

*Correspondence to:* Floriane Jamoteau ([floriane.jamoteau@unil.ch](mailto:floriane.jamoteau@unil.ch))

**Abstract.** Mineral-organic associations are crucial carbon and nutrient reservoirs in soils. However, soil cultivation disrupts these associations, leading to carbon loss and reduced soil fertility. Although, identifying the specific type(s) of mineral-organic associations susceptible to destruction or transformation upon cropping remains challenging, it is essential for devising  
10 strategies to preserve organic matter in croplands. Here we aimed to determine the predominant mineral-organic associations and to identify which types of associations are transformed upon cultivation. To achieve this, we sampled an andosol from both a forested and a cultivated area. We then analyzed cultivation-induced changes in soil physicochemical parameters and characterized mineral-organic associations using an array of spectro-microscopic techniques (TEM-EDX, TEM-EELS, and STXM), for comprehensive structural and compositional analysis. At the micro and nanoscale, we observed mineral-organic  
25 associations in the form of coprecipitates composed of amorphous oligomers containing Al, Si, and Fe (referred to as nanoCLICs for nanosized coprecipitates of inorganic oligomers with organics). Down to a few hundred nanometers, the nanoCLICs displayed elemental enrichments with C+Al+Si, C+Fe+Al+Si, or Al+Si dominance with less C. In contrast, organic matter exhibited various C speciation without compound-specific enrichments. These findings suggest that mineral-organic associations in andosols are nanoCLICs-type coprecipitates rather than organic matter associated solely with secondary  
30 minerals. NanoCLICs were present in both forest and crop andosols, and while cropping led to a 50% decrease in nanoCLICs, it did not alter their nature. This novel conceptualization of mineral-organic associations as nanoCLICs shifts our understanding of their persistence in andosols and demonstrates their vulnerability to crop-induced changes.

**Keywords:** Mineral-organic associations, cropland, land-use, andosol, nanoscale, transmission electron microscopy



## 35 1 Introduction

Carbon sequestration in terrestrial ecosystems is facilitated through protecting organic compounds within mineral-organic associations from microbial access (Cotrufo et al., 2019; Lugato et al., 2021). Beyond their contribution to carbon sequestration, these associations serve as crucial nutrient reserves for plants and soil microorganisms, thereby enhancing soil fertility, essential for maintaining agricultural productivity (Bernard et al., 2022; Fontaine et al., 2024). However, soil cultivation disrupts these mineral-organic associations, leading to significant loss C—a phenomenon known as ‘carbon destabilization’ (Sanderman et al., 2017; Bailey et al., 2019). In order to maintain agricultural productivity in cultivated soils, it is essential to preserve mineral-organic associations during transitions from natural to cultivated soils and to increase or maintain the remaining quantities in cultivated soils.

Mineral-organic associations have traditionally been regarded as resulting from organic matter adsorption onto mineral surfaces or coprecipitation with short-range order mineral phases. These short-range order phases include ferrihydrite, imogolites, and allophanes (Wagai and Mayer, 2007; Kleber et al., 2015; Basile-Doelsch et al., 2020; Kleber et al., 2021). Yet, this paradigm largely stems from indirect measurements of minerals rather than direct characterizations of the entire mineral-organic assemblage (e.g. using selective extractions; Rennert and Lenhardt, 2024). Recent advances in nanoscale (spectro)microscopy (e.g., TEM-EDX, STXM) have facilitated precise analyses of mineral-organic associations' composition and structure (Kinyangi et al., 2006; Solomon et al., 2007; Wan et al., 2007; Solomon et al., 2012; Asano et al., 2018), offering deeper insights into their stability under agricultural practices. In andosols, soils with high concentrations of mineral-organic associations, microscopy and spectroscopy approaches have refuted the stabilizing role of short-range order minerals for C (Levard et al., 2012). Instead, organic carbon is primarily associated in the form of nanosized coprecipitates of inorganic oligomers with organics (nanoCLICs), where organic molecules are linked to a few atoms of Al, Fe, or Si without crystalline structures (Tamrat et al., 2019; Jamoteau et al., 2023). These findings challenge previous assumptions about the types of mineral-organic associations in andosols developed from basalt parent material, suggesting a more amorphous constitution than earlier proposed models (Jamoteau et al., 2023). Different mechanisms may give rise to the formation of nanoCLICs in these soils: either Fe presence in soil solution (derived from mineral weathering) prevents Al and Si from assembling into short-range order minerals growth (imogolite and allophane), favoring nanoCLICs formation; or organic matter directly associates with amorphous phases over short-range order minerals. To investigate if nanoCLICs predominate mineral-organic associations in andosols, or if a combination of different types of mineral-organic associations including nanoCLICs and organic matter adsorbed on short-range ordered minerals are present, further characterization is required, especially in andosols developed on Fe-poor parent material.

In addition to characterizing existing mineral-organic associations, identifying the one vulnerable to destruction or transformation during cropping is crucial for developing strategies to preserve organic matter in croplands. Disruption of mineral-organic associations in crop soils can be attributed to multiple factors: (i) disruption of soil aggregates, releasing entrapped mineral-organic associations (Bailey et al., 2019; Derrien et al., 2023; Even and Cotrufo, 2024); (ii) intensified root



and microbial activities may accelerate mineral-organic associations disruption (Keiluweit et al., 2015; Jilling et al., 2021; Fontaine et al., 2024); or (iii) shifts in soil physicochemical parameters, notably pH, can weaken mineral-organic interactions (Newcomb et al., 2017; Bailey et al., 2019). However, the susceptibility of mineral-organic associations to destabilization varies, depending on mineral crystallinity and binding strength (Li et al., 2017; Newcomb et al., 2017; Bernard et al., 2022). Consequently, some associations could be more prone to disruption than others, potentially altering the types of remaining mineral-organic associations after long-term soil cropping. Although the underlying mechanisms are not fully understood, some evidence suggests that associations with lower mineral crystallinity are particularly prone to disruption and exhibit faster turnover (Li et al., 2017; Hall et al., 2018). In andosols, for instance, nanoCLICs-type mineral-organic associations, characterized by their amorphous mineral components composed of only a few atoms, could be particularly prone to disruption. Therefore, long-term cropping of andosols may lead to the disruption of nanoCLICs-type associations, which would significantly alter the type of remaining mineral-organic associations.

This study aims to determine the predominant mineral-organic associations within andosols and their vulnerability to carbon destabilization upon agricultural conversion. Specifically, we seek to determine if nanoCLICs are the prevalent form of mineral-organic associations within andosols, irrespective of their development on Fe-poor parent material, or if a combination of mineral-organic associations of different nature is instead present. Additionally, we aim to assess the impact of cropping on the type and abundance of mineral-organic associations in soil and if long-term cropping differently affects certain types of mineral-organic associations. Our working hypotheses posit that: (i) organic matter preferentially associates with amorphous mineral phases over short-range order minerals in andosols, thus making nanoCLICs the predominant mineral-organic associations in andosols; (ii) nanoCLICs are particularly prone to physicochemical transformations induced by cultivation, making them susceptible to destruction, and shifting the predominant mineral-organic association in cultivated andosol from nanoCLICs-type to mainly organic matter adsorb onto short-range order minerals. To probe these hypotheses, we sampled an andosol formed on a Fe-poor parent material (andesite rock). We conducted analyses on two andosol topsoil that are 300 m apart, one under forest and the other subjected to three decades of cultivation. We then identified cultivation-induced changes in physicochemical parameters and characterized mineral-organic associations by employing an array of spectro-microscopic techniques including TEM-EDX, TEM-EELS, and STXM for comprehensive structural and compositional analysis.

## 2 Material and methods

### 2.1 Soil sampling and fine fractions separation

Two andosol profiles (10-20 cm horizons) were sampled on La Martinique island (French West Indies). One profile was located under a forest (14°46'31" N; 61°2'31" W), while the other was situated 300 meters away in an area converted to agriculture 30 years ago (14°46'27" N; 61°2'57" W). Both profiles were situated at 300 meters above sea level, in a humid tropical climate (average temperature of 25°C and average annual precipitation of 3000 mm·year<sup>-1</sup>). The crop soil, converted



100 30 years ago, transitioned from a forest to a cropping system with 3-year rotations of taro, sweet potatoes, yams, and fallow periods. After sampling, the samples were kept humid at 4°C.

The fine fractions from both the forest and crop soil, primarily composed of C within mineral-organic associations, were isolated through wet sieving. Briefly, 10-20 g of air-dried soil was added to 100 mL of milliQ water and sonicated (16 J.mL<sup>-1</sup>). The 100 mL suspension was then wet sieved using a 20 µm mesh. After a minimum 12-hour settling period at 4°C of  
105 the < 20 µm fraction, the supernatant was removed, and the sedimented fraction was dried at 30°C.

## 2.2 Monitoring of cultivation-induced soil physico-chemical changes

The C content of bulk soils and fine fractions was analyzed using dry combustion with a Thermo FlashSmart elemental analyzer. The mineralogy of bulk soils and fine fractions was analyzed on free powder deposited on a silicon sample holder. This analysis was performed using an X-ray diffractometer (Co-K $\alpha$  source at 40 mA;  $\lambda = 1.79$ ; 2-75°; time step of  
110 0.033°, Philips P3710 X-ray). The quantity of poorly crystalline phases in bulk soils was quantified through sequential extractions using Na-pyrophosphate, ammonium oxalate-acid, and dithionite-citrate bicarbonate (Tamm, 1922; Pansu and Gautheyrou, 2006). After extractions, solubilized Fe, Al, and Si were measured using inductively coupled plasma atomic emission spectroscopy (ICP-AES).

## 2.3 Characterization of mineral-organic associations

### 115 2.3.1 Probing type of mineral-organic associations using TEM images and TEM-EDX and TEM-EELS chemical mappings

For microscopy analyses, fine fractions of the forest and the crop soil were isolated through sedimentation: 2g of soil was added to 35 mL of milliQ water and sonicated at low power to induce minimal disaggregation (16 J.mL<sup>-1</sup>; Just et al., 2021). After a minimum of 1 hour of sedimentation, the brown supernatant (with a gel-like texture) was collected and stored  
120 at 4°C. Before microscopy analysis, the suspension was diluted into ultrapure water (1/100), and 5 to 7 µL were deposited on copper grids coated with a lacey carbon film (porous film). The grids were air-dried for a few minutes before microscopy analysis. The analyses were performed using a transmission electron microscope (TEM) FEI Tecnai Osiris at 200 kV, coupled with an Energy-Dispersive X-ray spectroscopy (EDX) detection system (Super-X EDS). Imaging was conducted in bright field (direct beam) and dark field (annular dark field and high angular dark field; diffracted beam) mode. Chemical mapping was  
125 carried out using scanning transmission electron microscopy (STEM-EDX) and electron energy loss spectroscopy (TEM-EELS).

EDX Mapping was conducted with acquisition times varying from 15 to 90 minutes. The chemical mapping obtained through EDX was analyzed using Esprit software (version 1.9, Bruker), and atomic proportions (at.%) were determined using the PB-ZAF algorithm. STEM-EDX mapping allowed for atomic detections at scales ranging from hundred nanometers to  
130 micrometric scales. Twelve EDX mappings were carried out on the fine fractions of the forest soil, while 4 mappings were carried out on the fine fractions of the crop soil. From these mappings, various zones were selected to quantify atomic



proportions, ensuring micrometric representativeness (27 zones for the forest soil and 9 for the crop soil). To examine potential atomic composition heterogeneities among these zones, a principal component analysis of C, Fe, Al, and Si proportions followed by a k-means cluster analysis (with three imposed clusters) was performed on the selected zones using Rstudio software (using the ‘stats’, ‘ggplot2’, and ‘FactoMineR’ packages). Despite the lack of significant differences between the clusters, we have retained a 3 k-means clustering (with an imposed number of clusters) to illustrate the variability in atomic composition across areas.

To ensure elemental co-localizations of C with specific elements (Al, Si, and Fe) down to a few nanometers, TEM-EELS mappings were conducted on fine fractions of both forest and crop soils. These analyses followed protocols outlined in Jamoteau et al., (2023). Briefly, the energy range examined spanned the following edges: C K-edge (284 eV), O K-edge (532 eV), Fe L-edge (708 eV), Al K-edge (1560 eV), and Si K-edge (1839 eV). To minimize beam damage while ensuring precise elemental detection at the intended scales, the analysis time per pixel was kept as short as possible. EELS data collection occurred in two phases: initially from 250 to 1224 eV with a pixel analysis duration between 0.05 to 0.09 seconds; subsequently from 1,050 to 2,074 eV with an analysis time of 0.1-1.5 seconds per pixel. The compilation of nanoscale-resolved elemental co-localizations was executed using a Python script available in Jamoteau et al., (2023).

### 2.3.2. Probing organic matter types within mineral-organic associations using STXM

To investigate the types of organic matter within mineral-organic associations, elemental maps of C, Fe, and Al, along with speciation maps of C (K-edge), were analyzed using scanning transmission X-ray microscopy (STXM) on fine fractions of forest and crop andosols (see part 2.1 for details on fine fraction separation). For these mappings, the fine fractions were re-humidified with ultrapure water to form a paste consistency. This mixture was instantly frozen using liquid nitrogen, and 400-nm-thick sections were sliced at cryogenic temperature using a cryo-ultramicrotome (equipped with a diamond knife, Leica UC7). These sections were placed onto Si<sub>3</sub>N<sub>4</sub> windows (75 nm thick, 1x1 mm, 100 μm; AGS172-3T @ Oxford Instruments) and air-dried. STXM analyses took place at the SOLEIL synchrotron (France) on HERMES beamline, where energy calibration was conducted for C (using CO<sub>2</sub> at 2 mbar) and Fe (using Fe oxides). At the edges of C, Fe, and Al, transmitted photons were recorded every 50 nm across a 5 μm x 5 μm area. The acquisition time was set to 3 ms for C and Fe edges and 5 ms for the Al edge at intervals of 50 nm. The samples were first analyzed at the C K-edge with varying scan parameters: 1 eV increments between 274 and 281 eV; 0.125 eV increments between 282.125 and 292 eV; 0.353 eV increments between 292 and 304 eV; followed by increments of 10 eV between 314 and 334 eV. Subsequently, analyses at the Fe L-edge included scan parameters of 0.5 eV increments between 700 and 705 eV; 0.15 eV increments between 705.15 and 712 eV; and finally, increments of 0.5 eV between 712.5 and 730 eV. Lastly, at the Al K-edge, increments of 0.5 eV was used between 1570 and 1600 eV. Background (I<sub>0</sub>) measurements were taken concurrently with sample analysis in an adjacent area for all edges. The C, Al, and Fe maps resulted from energy subtractions at specific intervals: C at 291.35 - 275 eV; Fe at 709.3 - 700 eV; Al at 1588.8 - 1580.2 eV. Spectra from these zones were normalized using Athena software (version V0.9.26; Ravel and Newville, 2005). To assess variations in C speciation within the mappings, spectral principal component analysis of the C K-edge was performed



165 using Orange software (version 3.35.0). However, no statistically distinct clusters were identified in the results. Areas were then selected to illustrate the uniformity of C speciation across the maps.

### 3 Results

#### 3.1 Soil physicochemical parameters impacted by the forest-to-crop transition

In order to determine the impact of cropping, we compared key soil physicochemical parameters between the forest  
170 and crop andosol (Fig. 1). The results showed that, compared to the forest soil, the crop soil had a lower total C content, decreasing from 73 to 30 gC.kg<sup>-1</sup> and leading to a loss of 60% of total soil C. The C content in the fine fractions (<20 μm, Fig. 1), attributed to C in the form of mineral-organic associations (MOA), decreased from 49 to 23 gMOA-C.kg<sup>-1</sup>, indicating a 50% decrease in mineral-organic associations in the crop soil. Regarding mineralogy, both bulk and fine fractions of the forest and crop andosols exhibited the same mineral composition including pyroxenes, orthopyroxenes, plagioclases, titanomagnetite, quartz, and gibbsite, as well as poorly crystalline phases (analyzed by XRD, see SI1). However, quantitative  
175 analysis of amorphous and poorly crystalline phases using sequential extractions with pyrophosphate and oxalate (Rennert, 2018; Rennert and Lenhardt, 2024) showed differences between the forest and crop andosols. Al, Fe and Si extracted by pyrophosphate decreased by approximately 50 to 70% in the cultivated soil, indicating a quantitative reduction in amorphous mineral phases. Although no significant changes were observed in the elements extracted by oxalate targeting mostly short-  
180 range ordered minerals, dithionite extraction showed a reduction of approximately 20 to 40% for extracted Fe and Al in the crop soil, which can be attributed to a decrease in crystalline oxides. Compared to the forest soil, the crop soil hence quantitatively lost amorphous mineral phases and crystalline oxides. In addition, cropping also induced pH drop from 6.3 to 5.6. In summary, the comparative analysis of soil physicochemical parameters highlighted the effects of cultivation, which include a lower C content of the bulk soil and 50% less C in the form of mineral-organic associations, a decreased abundance  
185 of amorphous mineral phases, and a shift in the soil's physicochemical parameters, as indicated by the 0.7 pH decrease in the crop soil.

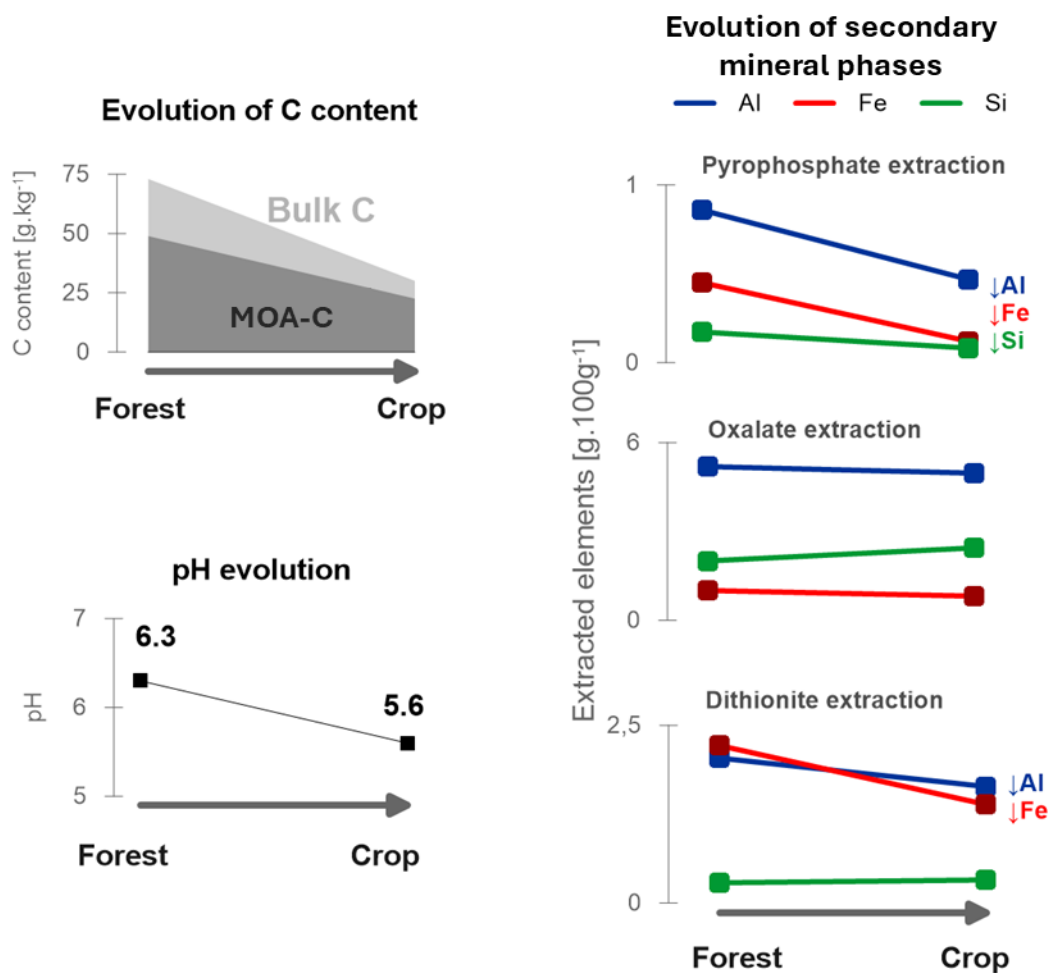


**Figure 1. Soil physicochemical parameters impacted by cropping.** Comparative analyses were conducted on bulk forest and crop andosols (at a depth of 10-15 cm), except for C content within mineral-organic associations (MOA-C), which was analyzed in the soil's fine fractions (<20 μm).



## 190 3.2 Probing type of mineral-organic associations in forest and crop soils

### 3.2.1 Mineral-organic associations in the form of coprecipitates

To identify the types of mineral-organic associations in forest and crop soils, we conducted chemical mappings using STEM-EDX (Fig. 2). These analyses confirmed previous mineralogical findings (from XRD diffractograms and sequential extractions) by identifying two distinct crystallographic phases: (1) crystalline mineral phases, ranging from a few hundred nanometers to micrometers in size, typically displaying rod-like shapes, and (2) an amorphous phase, likely in contact with the rod-like minerals (Fig. 2a and Fig. S2 for extra mappings). Across all mapped mineral-organic associations in both soil types, C was invariably found within the electron-amorphous phase (see Fig. 2A-B). Notably, C was never isolated; it consistently co-occurred with a mix of Al, Si and Fe in the electron-amorphous phase (Fig. 2C). This pattern was particularly noticeable in atomic proportions along the horizontal profile that sequentially crossed crystalline minerals (on the left side of the profile in Fig. 2D) and then amorphous phases (on the right side of the profile in Fig. 2D, see additional profiles in SI2), showing a marked C proportion increase upon entering and within the amorphous phase. These profiles, together with carbon mapping, demonstrated that C predominantly was located in the amorphous phase, closely associated with Al (~20%), Si (~15%), and to a lesser extent Fe (~3%). This nanoscale amorphous association of C with Al, Si, and Fe demonstrated that mineral-organic associations in both andosols were formed through the co-precipitation of elements derived from mineral weathering with organic matter, hereafter referred to as ‘coprecipitates’.



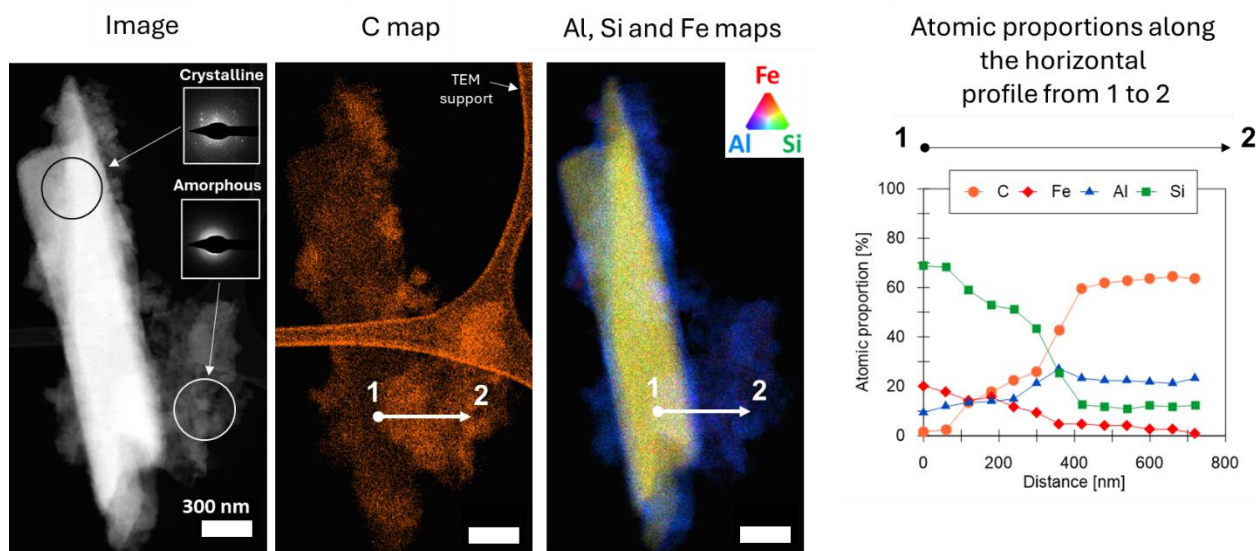


**Figure 2. Chemical mapping of mineral-organic associations using STEM-EDX.** These mappings were conducted on the fine fractions of the crop andosol. For the complete set of mineral-organic association mappings, refer to SI2. (A) TEM image in dark-field mode with electron-diffraction pattern in the boxes showing crystallinity of phases. (B) carbon mapping. (C) Fe, Si, Al mapping using RGB format; white arrow indicates the location of the 700 nm horizontal profile shown in D. (D) atomic proportions of C, Al, Si, Fe along the horizontal profile.



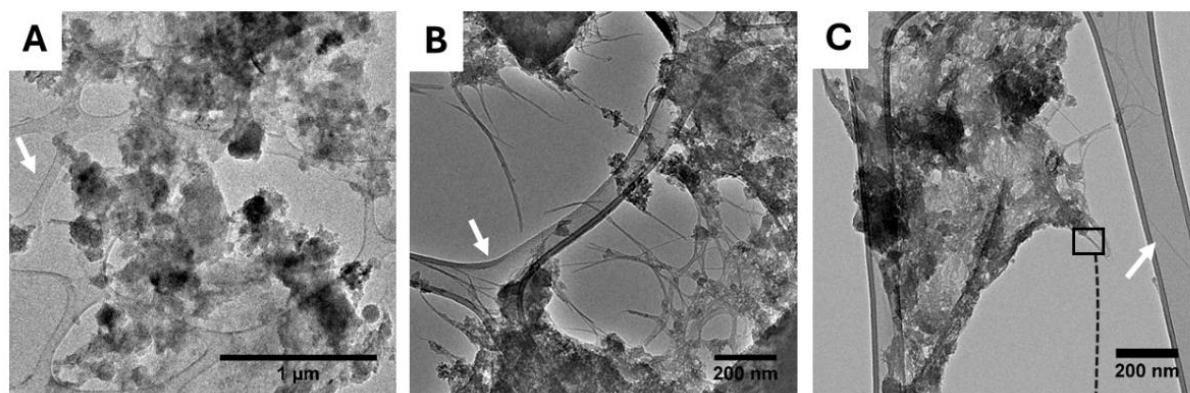
### 3.2.2 Nanoscale structure and composition of coprecipitates: nanoCLICs-type coprecipitates

210 To determine the composition and nanoscale structure of the amorphous phase containing coprecipitates, we  
conducted high-resolution transmission electron microscopy (HRTEM) to image the coprecipitates from micrometer to  
nanometer scales. Figure 3 presents six images from the forest soil, representative of all the acquired images from both soils  
(see SI3 for all HRTEM images). At the micrometer to sub-micrometer scale (Fig. 3A-C), we primarily observed aggregates  
and intertwined filaments. These filaments are indicative of imogolite, a short-range ordered mineral forming tubular structures  
215 of Al and Si, typically resulting from ash and pumice weathering (Wada, 1985; Wada and Harward, 1974; Parfitt, 2009; Levard  
and Basile Doelsch, 2016). At the nanometer scale (Fig. 2D-F), the aggregated phase primarily appeared amorphous, except  
for localized crystalline planes within the aggregates (as shown in Fig. 2E). The filaments have a diameter of about few  
nanometers (Fig. 3F), aligning with characteristics of imogolite or bundles of imogolites (Levard and Basile Doelsch, 2016),  
which were very fragile under the electron beam leading to amorphization of part of bundles. These results were observed  
220 across numerous distinct areas (see SI3) in both forest and crop soils. In sum, nanoscale images demonstrated that (1) the fine  
fractions were predominantly composed of amorphous phases and exhibited short-range order minerals typical of imogolite,  
and (2) the arrangement of forms with some crystallinity (such as small Fe or Al oxides) was observed but remains very minor  
in comparison to amorphous phases.

Then, to identify associated elements with C within the amorphous phase, 12 STEM-EDX mappings were conducted  
225 on the fine fraction from the forest soil and 4 mappings on the fine fraction from the crop soil. The results, consistent across  
both soils, demonstrated that C was predominantly colocalized with the amorphous phase in aggregate form (Fig. 4A-C, see  
SI4 for all mappings), with minimal presence on filamentous structures associated with imogolites (indicated by arrows in Fig.  
4A-C). Further STEM-EELS mappings confirmed nanoscale colocalization of C with Al, Si, and Fe within both forest and  
crop coprecipitates, observable below 15 nm scales (refer to SI5). These results indicated that the mineral component of  
230 coprecipitates is primarily composed of a mix of amorphous Al, Si, and Fe, even at scales down to 15 nm, and not composed  
of short-range ordered minerals like imogolite, allophane, and Fe-rich particles (e.i. ferrihydrite phases). The nanoscale  
colocalization of these elements (C, Al, Si, and Fe) demonstrates the presence of organic matter or organic molecules  
coprecipitated with inorganic oligomers (consisting of a few atoms) resulting from parent-andesite minerals weathering.  
Consequently, these coprecipitates are hereafter referred to as nanoCLICs-type of coprecipitates for nanosized coprecipitates  
235 of inorganic oligomers with organics (Tamrat et al., 2019).



### Micrometer scale TEM images



### Nanometer scale TEM images

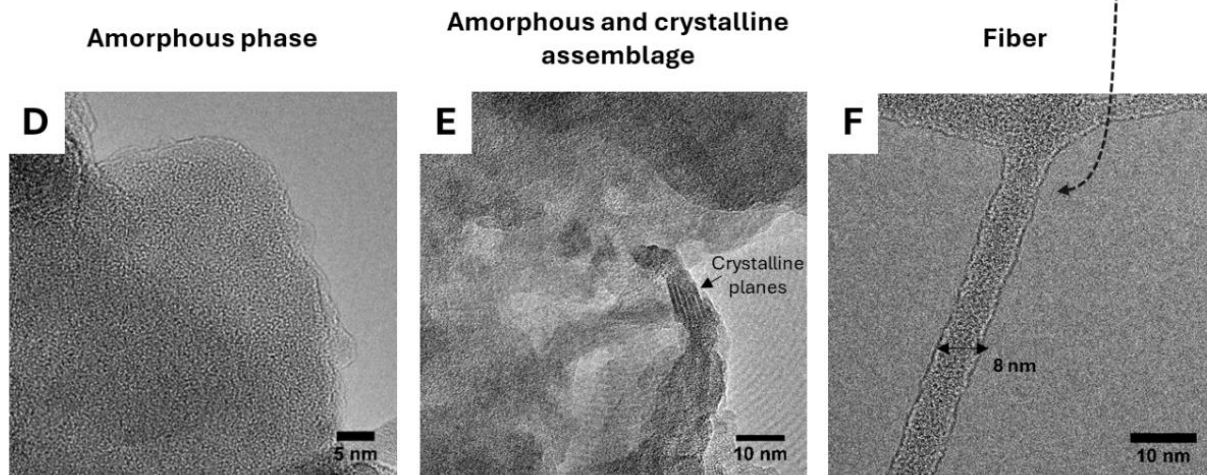
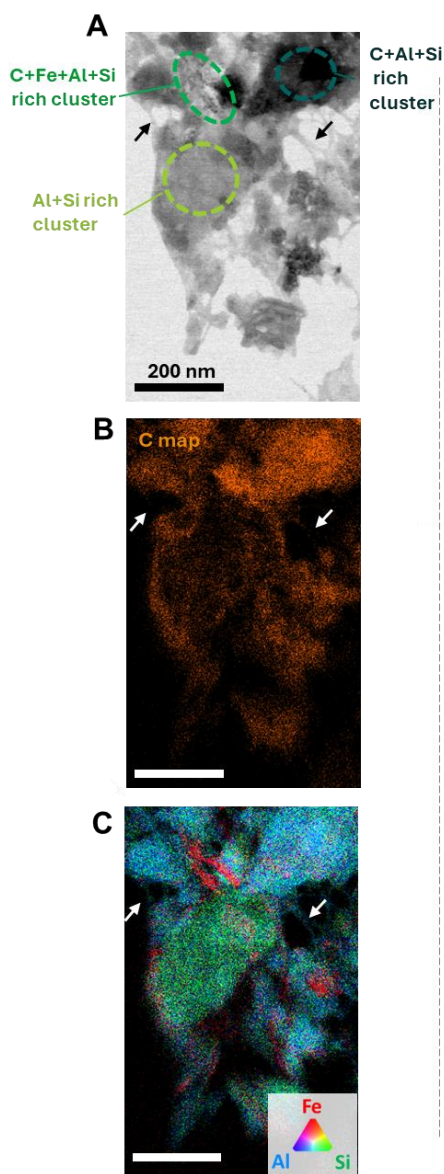


**Figure 3. High-resolution TEM analysis of the amorphous phase.** Microscale (A-C) and nanoscale (D-F) images of the amorphous aggregated phase and filaments. (D) Nanoscale image of the amorphous aggregated phase. (E) Localized crystallization within the aggregates (see crystalline planes). (F) Nanoscale image of an ~8 nm diameter filament, characteristic of imogolite minerals. The sample holder is denoted by the white arrow. These images were acquired on the fine fraction of the forest soil; for additional images in both soils, refer to SI3.

240

**Chemical mappings**



**Chemical proportions**

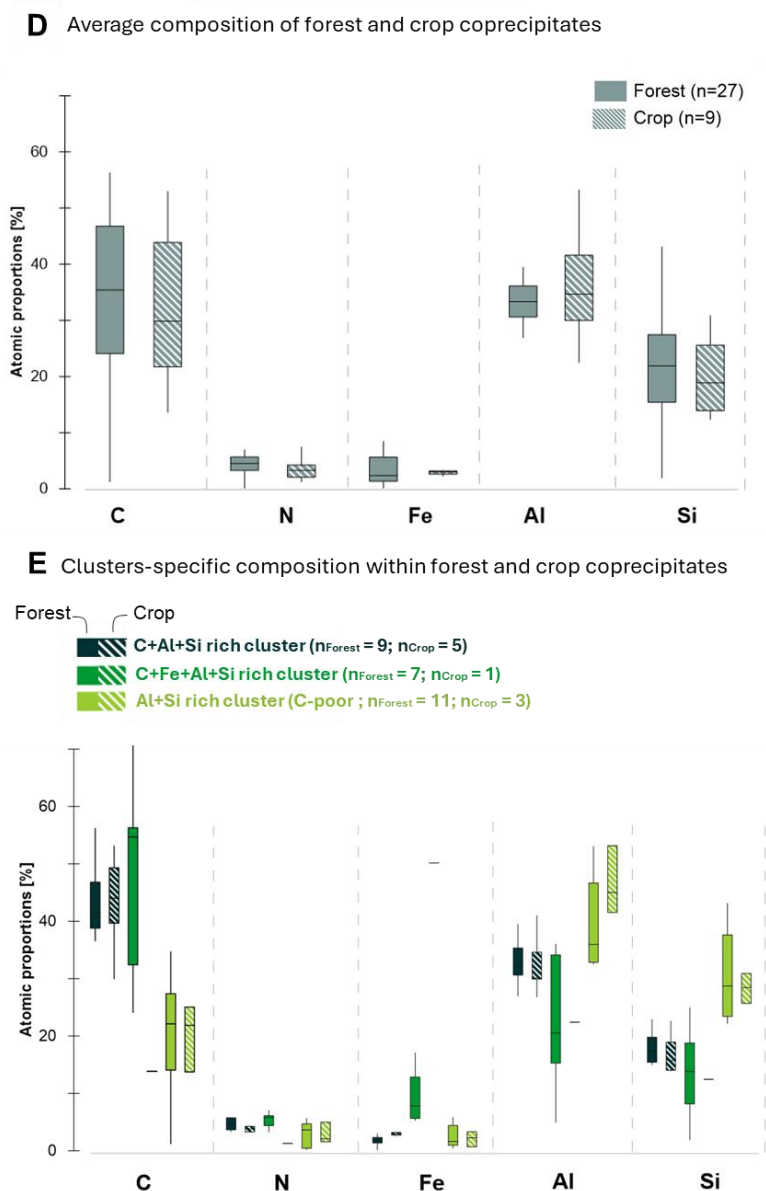


**Figure 4. Chemical mapping and atomic composition of forest and crop coprecipitates using STEM-EDX.** (A-C) chemical mapping of coprecipitates from the forest soil, see SI4 for additional mappings on forest and crop soils. (A) shows the imaged area, (B) display carbon detection, and (C) displays detections of Al, Si and Fe. Arrows indicate fibers characteristic of imogolites. (D) summarizes the average atomic proportions from selected areas across all mappings conducted on forest and crop soil coprecipitates, with ‘n’ representing the number of areas averaged. (E) details cluster-specific atomic proportions for clusters rich in C+Al+Si, C+Fe+Al+Si, as well as Al+Si (C poor), across various selected areas from all mappings on forest and crop soil coprecipitates. ‘n’ denotes the number of areas averaged. Examples of selected areas categorized as C+Al+Si, C+Fe+Al+Si, and Al+Si (C poor) are shown in (A).





### 3.2.3 Heterogeneity in the structure and composition of nanoCLICs-type coprecipitates

After characterizing nanoCLIC-type coprecipitates, we further investigate the structural and chemical composition heterogeneity between forest and crop coprecipitates. We selected various regions on nanoCLICs mappings and computed the atomic proportions within the selected area of  $\sim 100 \times 100$  nm (Fig. 4D-E, see SI4 for area localization on maps). Atomic proportions of these regions revealed comparable compositions of nanoCLICs in both forest and crop andosols (Fig. 4D). On average, nanoCLICs comprised 35% C, 4% N, 5% Fe, 34% Al, and 22% Si. However, these averaged proportions masked underlying heterogeneities in atomic proportion within the nanoCLICs. These include areas with high C+Al+Si proportions (averaging 44% C, 6% N, 2% Fe, 32% Al, and 17% Si), areas with high C+Fe+Al+Si proportions (44% C, 5% N, 14% Fe, 23% Al, and 13% Si), and areas with high Al+Si proportions but lower C proportion (21% C, 3% N, 2% Fe, 42% Al, and 32% Si; see Fig. 4E). Such heterogeneities were noted in both forest and crop coprecipitates (Fig. 4E), indicating a consistent variation in elemental proportions within the nanoCLICs.

Subsequently, to determine whether the nature of organic matter could affect these heterogeneities (i.e., selective associations with elemental mix of Al, Si and Fe), we conducted elemental mapping for C, Al and Fe using scanning transmission X-ray microscopy (STXM; see Fig. 5A) and assessed the elemental speciation of carbon through C K-edge analyses (Fig. 5B). The elemental mappings for C, Al and Fe corroborated the findings from STEM-EDX and STEM-EELS analyses: specifically, a dominant co-localization of C with Al (as indicated by the purple color in Fig. 5A), with heterogeneities in regions of a few hundred nanometers ( $\sim 500 \times 500$  nm), locally enriched in Fe (see areas 6, 7 and 8 in Fig. 5A), Al (area 5), or C (areas 3 and 4) observed in both forest and crop soils. Overall, C speciation results exhibited multiple peaks indicative of aromatic C=C and C=H ( $\sim 285$  eV), phenolic C-OH and ketonic C=O ( $\sim 286.6$  eV), carboxylic C=O and C-OH ( $\sim 288.4$  eV), and carbonyl C=O ( $\sim 290.4$  eV; Francis and Hitchcock, 1992; Cody et al., 1998; Boyce et al., 2002; Wan et al., 2007; Cosmidis and Benzerara, 2014; Le Guillou et al., 2018). Cluster analysis of the C K-edge did not reveal any distinct zones with different C speciation (SI6), nor did it indicate any differences in C speciation between nanoCLICs in forest and crop soils. Within the localized enriched area, a similar diversity of organic matter was detected in areas richer in C+Al+Fe (areas 1, 2, 8, 9), areas richer in C+Fe (areas 6, 7, 10), and areas richer in C+Al (area 5). Only the area enriched in C displayed distinct speciation, predominantly consisting of aromatic C=C and C=H ( $\sim 285$  eV) and carboxylic C=O and C-OH ( $\sim 288.4$  eV). These results, acquired in both forest and crop soils, indicated that a broad spectrum of organic molecules is coprecipitated within the nanoCLICs.



275

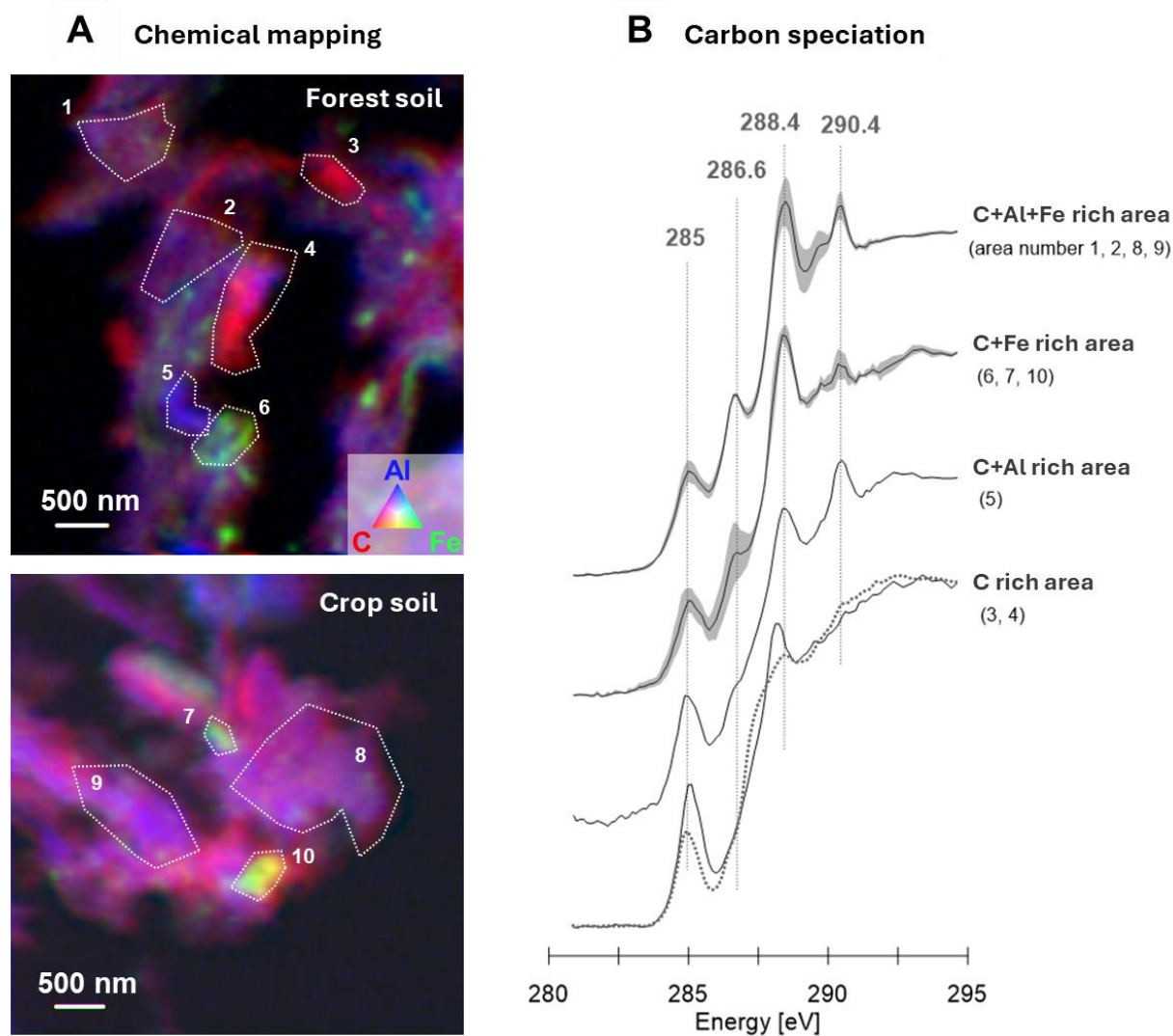


**Figure 5. Chemical mapping and organic matter characterization within coprecipitates using STXM mapping.** (A) STXM chemical mappings at the C K-edge, Fe L-edge, and Al K-edge of coprecipitates from forest and crop soils. (B) C K-edge spectra of the delineated area (outlined in panel A) showcase the principal energy bands associated with aromatic C=C and C=H (~285 eV), phenolic C-OH and ketonic C=O (~286.6 eV), carboxylic C=O and C-OH (~288.4 eV), and carbonyl C=O (~290.4 eV). C speciation exhibited consistency across the coprecipitates of both forest and crop soils (see individual spectra in SI6).



## 4 Discussion

### 4.1 Mineral-organic associations in andosols: in the form of nanoCLICs-type coprecipitates

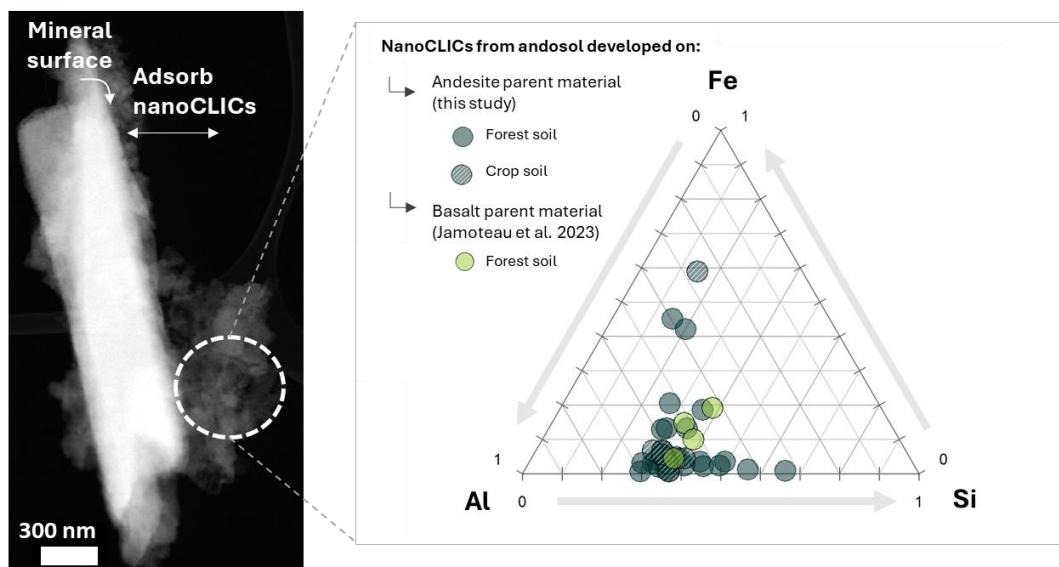
Mineral-organic associations are typically conceptualized as organic matter adsorbed or coprecipitated with secondary minerals (Kleber et al., 2015, 2021). In andosols, these associations are conceptualized as organic matter adsorbed on short-range ordered minerals like imogolite, allophane, and ferrihydrite (Wada and Harward, 1974; Wada, 1985; Kleber et al., 2004; Parfitt, 2009). However, certain andosols have been shown to lack these short-range ordered minerals (Levard et al., 2012), and nanoscale analyses revealed the presence of mineral-organic associations in the form of nanoCLICs (nanosized coprecipitates of inorganic oligomers with organics) instead of short-range order (this study and in Jamoteau et al., 2023). These nanoCLICs-type coprecipitates are more amorphous and heterogeneous than previously proposed, with their amorphous nature preserved by Si and organic matter that inhibit crystallization into short-range ordered minerals (Levard et al., 2012; Lenhardt et al., 2022, 2023). Confirming earlier observations of nanoCLICs in an andosol formed on basalt parent material (Jamoteau et al., 2023), our findings of nanoCLICs in an andosol developed on andesite parent material (an Fe-poor parent material) suggest that even in andosols with low Fe content in soil solutions—where short-range ordered minerals like imogolite can easily form (e.g., detection of imogolite, Fig 3 and 4)—the C is not localized with short-range ordered minerals but rather in the form of nanoCLICs with only oligomers of Al, Si and Fe. The presence of nanoCLICs suggests that organic matter preferentially associates with a mix a small oligomer ( $\pm\text{Al}$ ,  $\pm\text{Fe}$ ,  $\pm\text{Si}$ ) resulting from mineral weathering (weathering of primary and secondary minerals), rather than with short-range order minerals in andosols.

### 4.2 Heterogeneous chemical composition of nanoCLICs

In these nanoCLICs-type coprecipitates, our results showed an amorphous elemental mixture of C, Al, Si, and Fe. However, the proportions of these elemental mixtures showed enrichments in Al, Si, and/or Fe, with varying amounts of C, down to the hundred-nanometer scale (see Fig. 6A). The diversity of elemental composition within the nanoCLICs is illustrated in Fig. 6B, which displays (i) nanoCLICs richer in C+Al+Si, (ii) nanoCLICs richer in Al+Si (with less C), and (iii) nanoCLICs richer in C+Fe+Al+Si. This compositional heterogeneity in the mineral/inorganic portion of the nanoCLICs may arise from their formation in microsites with locally diverse elemental solutions. For instance, this could be influenced by the proximity to certain minerals that release specific elements into the soil solution, a process potentially controlled by microbial activity (Uroz et al., 2009; Bonneville et al., 2011, 2016). An alternative hypothesis for the compositional heterogeneity relates to the nature of organic matter, which might bind preferentially to certain elemental mixtures of Al, Si, and Fe. However, our findings refute this hypothesis by demonstrating consistent organic matter speciation across mappings, unrelated to nanoCLICs local enrichment in  $\pm\text{Al}$ ,  $\pm\text{Fe}$ , or  $\pm\text{Si}$  down to the hundred-nanometer scale (Fig. 5). The same diversity of organic matter, composed of aromatic-C, phenolic-C, ketonic-C, carboxylic-C, and carbonyl-C, is present across all maps and within subregions (Fig. 5). This finding aligns with similar diversity observed in mineral-organic associations from various temperate and tropical soils, despite distinct vegetation compositions and soil mineralogy (Kinyangi et al., 2006; Lehmann et



## A Heterogeneous composition of nanoCLICs



## B Conceptual model of nanoCLICs structure and composition

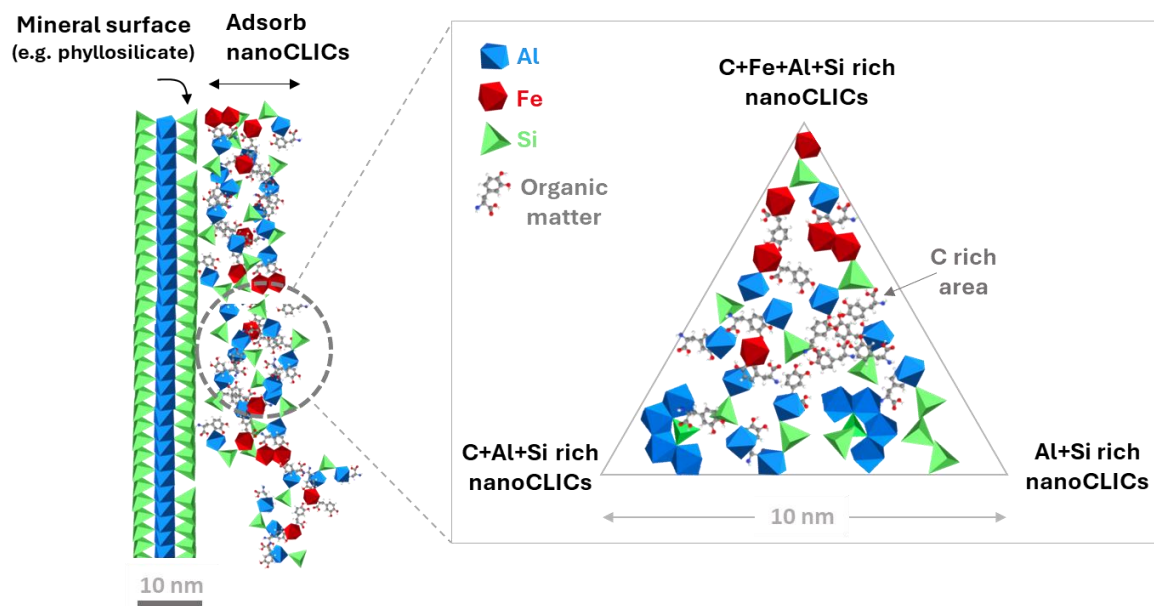


**Figure 6. Structure and composition of nanoCLICs in andosols.** (A) atomic proportions of nanoCLICs-type coprecipitates in andosols developed on andesite parent material (current study) compared to andosols developed on basalt parent material (Jamoteau et al., 2023). Atomic proportions are based on STEM-EDX mappings. (B) Schematic representation of nanoCLICs adsorbed on a mineral surface (a 2:1 phyllosilicate as an example) and a ternary diagram illustrating the compositional heterogeneity of nanoCLICs.





al., 2008; Solomon et al., 2012; Asano et al., 2018). Consequently, a broad spectrum of organic matter can form mineral-  
310 organic associations, including nanoCLIC-type associations. The only significant speciation difference was noted in areas  
enriched in C, characterized by an increase in aromatic and carboxylic C (Fig. 5, zones 3 and 4). The enrichment in aromatic-  
C in areas where C is not associated with other elements aligns with findings in other soil types (Solomon et al., 2012; Lutfalla  
et al., 2019), and may stem from the presence of particulate organic matter, thus indicating less degraded organic matter in  
these areas than within the nanoCLICs.

#### 315 **4.3 Adsorption of nanoCLICs on mineral surfaces**

In prevailing conceptual frameworks of mineral-organic associations, two dominant paradigms are recognized:  
coprecipitation and adsorption of organic matter with minerals (Kleber et al., 2015, 2021). Our investigations reveal that  
nanoCLICs represent the main form of mineral-organic associations in andosols. However, adsorption mechanisms were also  
observed: adsorption of nanoCLICs onto mineral surfaces (Fig. 2) or through intercalation within phyllosilicate layers (refer  
320 to Fig. SI2). Our findings suggest that nanoCLICs-type coprecipitation processes likely occur either upstream or  
simultaneously with adsorption processes on mineral surfaces. These processes can take place in soil solutions, which contain  
both organic compounds and elements resulting from mineral weathering (such as Si, Al, Fe, Ca, and Mn; Campbell et al.,  
1989; Giesler and Lundström, 1993; Manderscheid and Matzner, 1995; Strobel et al., 2001; Kaiser et al., 2002). Coprecipitation  
and subsequent adsorption on mineral surfaces are, therefore, interrelated phenomena. Mineral-organic associations need to  
325 be conceptualized as a sum of different interactions rather than a single interaction. This study highlights this paradigm shift,  
with nanoCLICs coprecipitates being adsorbed onto mineral surfaces, thereby illustrating the complexity of mineral-organic  
associations assemblages in soils.

#### **4.4 Land-use change: a loss of nanoCLICs rather than changes in mineral-organic association types**

The transition from natural to cultivated soils typically results in a C stock decline (Poeplau and Don, 2013; Sanderman  
330 et al., 2017). In the studied andosol, which was converted for agricultural use 30 years ago, we observe a 60% reduction in C  
content, consistent with previous findings in the literature (Poeplau and Don, 2013). This substantial C depletion, with 50%  
attributable to the loss of C in the form of mineral-organic associations, underscores the destabilizing effect of agricultural  
practices on C. However, cultivation did not modify the type of mineral-organic associations present in the studied andosol.  
Both andosols exhibit nanoCLIC-type coprecipitates characterized by similar inorganic structural heterogeneity and organic  
335 matter diversity (Fig.4-5). Nanoscale examination revealed no discernible differences in nanoCLICs from the forest and the  
crop andosol. However, pyrophosphate extractions highlighted a marked reduction (50-70%) in extracted Al, Si, and Fe—  
suggestive of a decrease in amorphous and poorly crystalline soil minerals (Rennert, 2018; Rennert and Lenhardt, 2024). In  
this context, these extractions must target the nanoCLICs and imogolites observed at nanoscales (Fig. 4). The simultaneous  
reduction in C within mineral-organic associations and the overall quantity of amorphous elements suggests a decrease in  
340 nanoCLICs abundance. Furthermore, although the total C content in the cultivated soil has diminished, the relative C



proportion within the nanoCLICs remained constant, further indicating a reduction in nanoCLICs amount and not only the C content within the nanoCLICs. The subsequent fate of Al, Si, and Fe post-disassociation remains undetermined; these elements may undergo leaching or transition into more crystalline structures undetectable by the sequential extraction methods used in this study. Ultimately, our findings suggest that agricultural activity predominantly affects the quantity rather than the type of  
345 mineral-organic associations in andosols.

#### 4.5 Insights into the stability of mineral-organic associations in andosols

In the literature, mineral-organic associations within andosols are considered to be stable across extensive centennial durations, with radiocarbon dating revealing persistence into the millennial range (Shimada et al., 2022). Contrary to this prevailing view, our results suggest that these mineral-organic associations, characterized as nanoCLICs-type coprecipitates,  
350 are prone to destabilization post three decades of agricultural activity. This indicates that while such associations may persist for a long time within certain andosols, they are susceptible to disruption contingent upon cultivation. The observed loss after cultivation could be attributed to the disruption of amorphous mineral constituents of nanoCLICs—namely Al, Si, and Fe—given that amorphous Al and Fe exhibit diminished stability under reduced pH conditions. Consequently, nanoCLICs may experience partial solubilization as a result of the pH diminution in the crop soil, leading to the loss of these associations. Even  
355 though there was a total pH decrease of about one unit, from 6.3 to 5.6 (Fig. 1), this overall reduction could reflect stronger local decreases, possibly caused by root exudates and the biological activity (Keiluweit et al., 2015; Bernard et al., 2022), leading to nanoCLICs disruption. Moreover, given the heterogeneous composition of nanoCLICs (Fig. 4), their transformations may vary based on local composition. For example, nanoCLICs with a high Fe content may exhibit increased sensitivity to redox fluctuations and pH decreases, while those enriched with Al and Si may show sensitivity to pH decreases. Such  
360 compositional-dependent transformations were not found in our results, which demonstrated consistent heterogeneity of nanoCLICs across both forest and crop andosols (Fig. 4). In addition to their chemical vulnerability to physicochemical changes, agricultural soil management practices might also play a role in nanoCLICs disruption. Soil disturbance during cultivation lessens aggregate occlusion, enhancing interaction between the microbial community, roots, and nanoCLICs, which could lead to their destruction (Bailey et al., 2019). Consequently, this study showed that nanoCLICs-type mineral-organic  
365 associations is susceptible to disruption upon cultivation.

#### Conclusion

The micro and nanoscale characterization of mineral-organic associations within andosols demonstrated the presence of nanoCLICs-type coprecipitates, for nanosized coprecipitates of inorganic oligomers with organic molecules. These nanoCLICs, observed in both forested and cultivated andosols, exhibited an amorphous composition and chemical  
370 heterogeneity, challenging prior conceptions of mineral-organic associations in andosols. The mineral constituents of these coprecipitates were composed of amorphous oligomers, made of a mixture of Fe, Al, and Si in varying atomic proportions,



including zones with a dominance of either C+Al+Si, C+Fe+Al+Si, or C-poor nanoCLICs richer in Al+Si. The organic matter composition of nanoCLICs was diverse, made of aromatic-C, phenolic-C, ketonic-C, carboxylic-C and carbonyl-C, suggesting the potential for nanoCLICs formation with various types of organic matter. These insights reconsider the nature of mineral-organic associations in andosols as nanoCLICs-type coprecipitates rather than solely organic matter associated with secondary imogolite-type minerals. Furthermore, our spatial mapping suggests that these nanoCLICs-type coprecipitates may adhere to mineral surfaces, suggesting that such associations are a composite of multiple interaction types rather than a singular form. While the presence of nanoCLICs in both forest and crop andosols is confirmed, it is noteworthy that cultivation has led to a significant loss, over 50%, of total C within nanoCLICs, alongside notable physicochemical alterations, including a pH reduction by one unit. These changes did not alter the nature of mineral-organic associations but rather reduced the abundance of nanoCLICs. This novel conceptualization of mineral-organic associations as nanoCLICs in andosols, and their susceptibility to agricultural practices, shifts our understanding of mineral-organic associations persistence in andosols.

#### **Data availability**

Data are available upon request from the corresponding author.

#### **Author contributions**

F.J. contributed to conceptualization, methodology, formal analysis, and writing – original draft. E.D. participated in conceptualization, methodology, formal analysis, writing – review and editing. N.C. and C.L. were involved in conceptualization, methodology, and formal analysis, writing – review and editing. T.W., F.S.A., S.S, A.D., D.B., M.L.P., P.C., V.V., and N.B. contributed to sampling, methodology, and formal analysis. I.D.B. participated in conceptualization, methodology, formal analysis, and writing - review and editing.

#### **Competing interests**

The authors declare that they have no conflict of interest.

#### **Acknowledgments**

The author thanks the research funding partners: ANR (NanoSoilC project ANR-16-CE01-0012-02), the Equipex nanoID platform (2010-2019), la Région SUD and CIRAD (Emploi Jeunes Doctorants, subvention n°2019\_03559, DEB 19-574). The author thanks Stefan Stanescu for his support during analyses on the HERMES beamline at the Soleil synchrotron and Marco Keiluweit for his edits to the manuscript. The author thanks PiCSL-FBI core platform (IBDM, AMU-Marseille, member of the France-BioImaging national research infrastructure, ANR-10-INBS-04), where the cryo-sections were conducted.



## 400 References

- Asano, M., Wagai, R., Yamaguchi, N., Takeichi, Y., Maeda, M., Suga, H., Takahashi, Y., 2018. In Search of a Binding Agent: Nano-Scale Evidence of Preferential Carbon Associations with Poorly-Crystalline Mineral Phases in Physically-Stable, Clay-Sized Aggregates. *Soil Syst.* 2, 32. <https://doi.org/10.3390/soilsystems2020032>
- 405 Bailey, V.L., Pries, C.H., Lajtha, K., 2019. What do we know about soil carbon destabilization? *Environ. Res. Lett.* 14, 083004. <https://doi.org/10.1088/1748-9326/ab2c11>
- Basile-Doelsch, I., Balesdent, J., Pellerin, S., 2020. Reviews and syntheses: The mechanisms underlying carbon storage in soil. *Biogeosciences Discuss.* 1–33. <https://doi.org/10.5194/bg-2020-49>
- Bernard, L., Basile-Doelsch, I., Derrien, D., Fanin, N., Fontaine, S., Guenet, B., Karimi, B., Marsden, C., Maron, P.-A., 2022. Advancing the mechanistic understanding of the priming effect on soil organic matter mineralisation. *Funct. Ecol.* n/a. <https://doi.org/keilukey>
- 410 Bonneville, S., Bray, A.W., Benning, L.G., 2016. Structural Fe(II) Oxidation in Biotite by an Ectomycorrhizal Fungi Drives Mechanical Forcing. *Environ. Sci. Technol.* 50, 5589–5596. <https://doi.org/10.1021/acs.est.5b06178>
- Bonneville, S., Morgan, D.J., Schmalenberger, A., Bray, A., Brown, A., Banwart, S.A., Benning, L.G., 2011. Tree-mycorrhiza symbiosis accelerate mineral weathering: Evidences from nanometer-scale elemental fluxes at the hypha–mineral interface. *Geochim. Cosmochim. Acta* 75, 6988–7005. <https://doi.org/10.1016/j.gca.2011.08.041>
- 415 Boyce, C.K., Cody, G.D., Feser, M., Jacobsen, C., Knoll, A.H., Wirick, S., 2002. Organic chemical differentiation within fossil plant cell walls detected with X-ray spectromicroscopy. *Geology* 30, 1039–1042. [https://doi.org/10.1130/0091-7613\(2002\)030<1039:OCDWFP>2.0.CO;2](https://doi.org/10.1130/0091-7613(2002)030<1039:OCDWFP>2.0.CO;2)
- Campbell, D.J., Kinniburgh, D.G., Beckett, P.H.T., 1989. The soil solution chemistry of some Oxfordshire soils: temporal and spatial variability. *J. Soil Sci.* 40, 321–339. <https://doi.org/10.1111/j.1365-2389.1989.tb01277.x>
- 420 Cody, G.D., Ade, H., Wirick, S., Mitchell, G.D., Davis, A., 1998. Determination of chemical-structural changes in vitrinite accompanying luminescence alteration using C-NEXAFS analysis. *Org. Geochem.* 28, 441–455. [https://doi.org/10.1016/S0146-6380\(98\)00010-2](https://doi.org/10.1016/S0146-6380(98)00010-2)
- Cosmidis, J., Benzerara, K., 2014. Soft x-ray scanning transmission spectromicroscopy, in: *Biomineralization Sourcebook*. CRC Press.
- 425 Cotrufo, M.F., Ranalli, M.G., Haddix, M.L., Six, J., Lugato, E., 2019. Soil carbon storage informed by particulate and mineral-associated organic matter. *Nat. Geosci.* 12, 989–994. <https://doi.org/10.1038/s41561-019-0484-6>
- Derrien, D., Barré, P., Basile-Doelsch, I., Cécillon, L., Chabbi, A., Crème, A., Fontaine, S., Henneron, L., Janot, N., Lashermes, G., Quéneá, K., Rees, F., Dignac, M.-F., 2023. Current controversies on mechanisms controlling soil carbon storage: implications for interactions with practitioners and policy-makers. A review. *Agron. Sustain. Dev.* 43, 21. <https://doi.org/10.1007/s13593-023-00876-x>
- 430 Even, R.J., Cotrufo, M.F., 2024. The ability of soils to aggregate, more than the state of aggregation, promotes protected soil organic matter formation. *Geoderma* 442, 116760. <https://doi.org/10.1016/j.geoderma.2023.116760>
- Fontaine, S., Abbadie, L., Aubert, M., Barot, S., Bloor, J.M.G., Derrien, D., Duchene, O., Gross, N., Henneron, L., Le Roux, X., Loeuille, N., Michel, J., Recous, S., Wipf, D., Alvarez, G., 2024. Plant–soil synchrony in nutrient cycles: Learning from ecosystems to design sustainable agrosystems. *Glob. Change Biol.* 30, e17034. <https://doi.org/10.1111/gcb.17034>
- 435 Francis, J.T., Hitchcock, A.P., 1992. Inner-shell spectroscopy of p-benzoquinone, hydroquinone, and phenol: distinguishing quinoid and benzenoid structures. *J. Phys. Chem.* 96, 6598–6610. <https://doi.org/10.1021/j100195a018>
- 440 Giesler, R., Lundström, U., 1993. Soil Solution Chemistry: Effects of Bulking Soil Samples. *Soil Sci. Soc. Am. J.* 57, 1283–1288. <https://doi.org/10.2136/sssaj1993.03615995005700050020x>
- Hall, S.J., Berhe, A.A., Thompson, A., 2018. Order from disorder: do soil organic matter composition and turnover co-vary with iron phase crystallinity? *Biogeochemistry* 140, 93–110. <https://doi.org/10.1007/s10533-018-0476-4>
- Jamoteau, F., Cam, N., Levard, C., Doelsch, E., Gassier, G., Duvivier, A., Boulineau, A., Saint-Antonin, F., Basile-Doelsch, I., 2023. Structure and Chemical Composition of Soil C-Rich Al–Si–Fe Coprecipitates at Nanometer Scale. *Environ. Sci. Technol.* <https://doi.org/10.1021/acs.est.3c06557>
- 445 Jilling, A., Keiluweit, M., Gutknecht, J.L.M., Grandy, A.S., 2021. Priming mechanisms providing plants and microbes access to mineral-associated organic matter. *Soil Biol. Biochem.* 158, 108265. <https://doi.org/10.1016/j.soilbio.2021.108265>



- 450 Just, C., Poeplau, C., Don, A., van Wesemael, B., Kögel-Knabner, I., Wiesmeier, M., 2021. A Simple Approach to Isolate Slow and Fast Cycling Organic Carbon Fractions in Central European Soils—Importance of Dispersion Method. *Front. Soil Sci.* 1, 13. <https://doi.org/10.3389/fsoil.2021.692583>
- Kaiser, K., Guggenberger, G., Haumaier, L., Zech, W., 2002. The composition of dissolved organic matter in forest soil solutions: changes induced by seasons and passage through the mineral soil. *Org. Geochem.* 33, 307–318. [https://doi.org/10.1016/S0146-6380\(01\)00162-0](https://doi.org/10.1016/S0146-6380(01)00162-0)
- 455 Keiluweit, M., Bougoure, J.J., Nico, P.S., Pett-Ridge, J., Weber, P.K., Kleber, M., 2015. Mineral protection of soil carbon counteracted by root exudates. *Nat. Clim. Change* 5, 588–595. <https://doi.org/10.1038/nclimate2580>
- Kinyangi, J., Solomon, D., Liang, B., Lerotic, M., Wirick, S., Lehmann, J., 2006. Nanoscale Biogeocomplexity of the Organomineral Assemblage in Soil. *Soil Sci. Soc. Am. J.* 70, 1708–1718. <https://doi.org/10.2136/sssaj2005.0351>
- 460 Kleber, M., Bourg, I.C., Coward, E.K., Hansel, C.M., Myneni, S.C.B., Nunan, N., 2021. Dynamic interactions at the mineral–organic matter interface. *Nat. Rev. Earth Environ.* 2, 402–421. <https://doi.org/10.1038/s43017-021-00162-y>
- Kleber, M., Eusterhues, K., Keiluweit, M., Mikutta, C., Mikutta, R., Nico, P.S., 2015. Chapter One - Mineral–Organic Associations: Formation, Properties, and Relevance in Soil Environments, in: Sparks, D.L. (Ed.), *Advances in Agronomy*. Academic Press, pp. 1–140. <https://doi.org/10.1016/bs.agron.2014.10.005>
- Kleber, M., Mikutta, C., Jahn, R., 2004. Andosols in Germany—pedogenesis and properties. *CATENA, Volcanic Soil Resources: Occurrence, Development and Properties* 56, 67–83. <https://doi.org/10.1016/j.catena.2003.10.015>
- 465 Le Guillou, C., Bernard, S., De la Pena, F., Le Brech, Y., 2018. XANES-Based Quantification of Carbon Functional Group Concentrations. *Anal. Chem.* 90, 8379–8386. <https://doi.org/10.1021/acs.analchem.8b00689>
- Lehmann, J., Solomon, D., Kinyangi, J., Dathe, L., Wirick, S., Jacobsen, C., 2008. Spatial complexity of soil organic matter forms at nanometre scales. *Nat. Geosci.* 1, 238–242. <https://doi.org/10.1038/ngeo155>
- 470 Lenhardt, K.R., Breitzke, H., Buntkowsky, G., Mikutta, C., Rennert, T., 2022. Interactions of dissolved organic matter with short-range ordered aluminosilicates by adsorption and co-precipitation. *Geoderma* 423, 115960. <https://doi.org/10.1016/j.geoderma.2022.115960>
- Lenhardt, K.R., Stein, M., Rennert, T., 2023. Silicon Incorporation Reduces the Reactivity of Short-range Ordered Aluminosilicates Toward Organic Acids. *Clays Clay Miner.* <https://doi.org/10.1007/s42860-023-00248-2>
- 475 Levard, C., Basile Doelsch, I., 2016. Geology and mineralogy of imogolite-type materials, in: *Nanosized Tubular Clay Minerals, Developments in Clay Science*. Elsevier, Academic Press, p. np. <https://doi.org/10.1016/B978-0-08-100293-3.00003-0>
- Levard, C., Doelsch, E., Basile-Doelsch, I., Abidin, Z., Miche, H., Masion, A., Rose, J., Borschneck, D., Bottero, J.-Y., 2012. Structure and distribution of allophanes, imogolite and proto-imogolite in volcanic soils. *Geoderma* 183–184, 100–108. <https://doi.org/10.1016/j.geoderma.2012.03.015>
- 480 Li, H., Bölscher, T., Winnick, M., Tfaily, M.M., Cardon, Z.G., Keiluweit, M., 2017. Simple Plant and Microbial Exudates Destabilize Mineral-Associated Organic Matter via Multiple Pathways. *Environ. Sci. Technol.* 55, 3389–3398. <https://doi.org/10.1021/acs.est.0c04592>
- Lugato, E., Lavalley, J.M., Haddix, M.L., Panagos, P., Cotrufo, M.F., 2021. Different climate sensitivity of particulate and mineral-associated soil organic matter. *Nat. Geosci.* 14, 295–300. <https://doi.org/10.1038/s41561-021-00744-x>
- 485 Lutfalla, S., Barré, P., Bernard, S., Le Guillou, C., Alléon, J., Chenu, C., 2019. Multidecadal persistence of organic matter in soils: multiscale investigations down to the submicron scale. *Biogeosciences* 1401–1410.
- Manderscheid, B., Matzner, E., 1995. Spatial heterogeneity of soil solution chemistry in a mature Norway spruce (*Picea abies* (L.) Karst.) stand. *Water, Air, Soil Pollut.* 85, 1185–1190. <https://doi.org/10.1007/BF00477142>
- 490 Newcomb, C.J., Qafoku, N.P., Grate, J.W., Bailey, V.L., Yoreo, J.J.D., 2017. Developing a molecular picture of soil organic matter–mineral interactions by quantifying organo–mineral binding. *Nat. Commun.* 8, 396. <https://doi.org/10.1038/s41467-017-00407-9>
- Pansu, M., Gautheyrou, J. (Eds.), 2006. Mineralogical Separation by Selective Dissolution, in: *Handbook of Soil Analysis: Mineralogical, Organic and Inorganic Methods*. Springer Berlin Heidelberg, Berlin, Heidelberg, pp. 167–219. [https://doi.org/10.1007/978-3-540-31211-6\\_6](https://doi.org/10.1007/978-3-540-31211-6_6)
- 495 Parfitt, R.L., 2009. Allophane and imogolite: role in soil biogeochemical processes. *Clay Miner.* 44, 135–155. <https://doi.org/10.1180/claymin.2009.044.1.135>





- Poeplau, C., Don, A., 2013. Sensitivity of soil organic carbon stocks and fractions to different land-use changes across Europe. *Geoderma* 192, 189–201. <https://doi.org/10.1016/j.geoderma.2012.08.003>
- 500 Ravel, B., Newville, M., 2005. ATHENA, ARTEMIS, HEPHAESTUS: data analysis for X-ray absorption spectroscopy using IFEFFIT. *J. Synchrotron Radiat.* 12, 537–541. <https://doi.org/10.1107/S0909049505012719>
- Rennert, T., 2018. Wet-chemical extractions to characterise pedogenic Al and Fe species – a critical review. *Soil Res.* 57, 1–16. <https://doi.org/10.1071/SR18299>
- 505 Rennert, T., Lenhardt, K.R., 2024. Potential pitfalls when using popular chemical extractions to characterize Al- and Fe-containing soil constituents. *J. Plant Nutr. Soil Sci.* [jpln.202300268](https://doi.org/10.1002/jpln.202300268). <https://doi.org/10.1002/jpln.202300268>
- Sanderman, J., Hengl, T., Fiske, G., 2017. Soil carbon debt of 12,000 years of human land use. *Proc. Natl. Acad. Sci.* <https://doi.org/10.1073/pnas.1706103114>
- Shimada, H., Wagai, R., Inoue, Y., Tamura, K., Asano, M., 2022. Millennium timescale carbon stability in an Andisol: How persistent are organo-metal complexes? *Geoderma* 417, 115820. <https://doi.org/10.1016/j.geoderma.2022.115820>
- 510 Solomon, D., Lehmann, J., Harden, J., Wang, J., Kinyangi, J., Heymann, K., Karunakaran, C., Lu, Y., Wirrick, S., Jacobsen, C., 2012. Micro- and nano-environments of carbon sequestration: Multi-element STXM–NEXAFS spectromicroscopy assessment of microbial carbon and mineral associations. *Chem. Geol., Looking into the Nano-World using X-Rays* 329, 53–73. <https://doi.org/10.1016/j.chemgeo.2012.02.002>
- 515 Solomon, D., Lehmann, J., Kinyangi, J., Amelung, W., Lobe, I., Pell, A., Riha, S., Ngoze, S., Verchot, L., Mbugua, D., Skjemstad, J., Schäfer, T., 2007. Long-term impacts of anthropogenic perturbations on dynamics and speciation of organic carbon in tropical forest and subtropical grassland ecosystems. *Glob. Change Biol.* 13, 511–530. <https://doi.org/10.1111/j.1365-2486.2006.01304.x>
- Strobel, B.W., Hansen, H.C.B., Borggaard, O.K., Andersen, M.K., Raulund-Rasmussen, K., 2001. Composition and reactivity of DOC in forest floor soil solutions in relation to tree species and soil type. *Biogeochemistry* 56, 1–26. <https://doi.org/10.1023/A:1011934929379>
- 520 Tamm, O., 1922. Eine Methode zur Bestimmung der anorganischen Komponenten des Gelkomplexes im Boden. *Medd. Fran Statens Skogsforsöksanstalt* 19, 385–404.
- Tamrat, W.Z., Rose, J., Grauby, O., Doelsch, E., Levard, C., Chaurand, P., Basile-Doelsch, I., 2019. Soil organo-mineral associations formed by co-precipitation of Fe, Si and Al in presence of organic ligands. *Geochim. Cosmochim. Acta* 260, 15–28. <https://doi.org/10.1016/j.gca.2019.05.043>
- 525 Uroz, S., Calvaruso, C., Turpault, M.-P., Frey-Klett, P., 2009. Mineral weathering by bacteria: ecology, actors and mechanisms. *Trends Microbiol.* 17, 378–387. <https://doi.org/10.1016/j.tim.2009.05.004>
- Wada, K., 1985. The Distinctive Properties of Andosols, in: Stewart, B.A. (Ed.), *Advances in Soil Science, Advances in Soil Science*. Springer New York, pp. 173–229.
- 530 Wada, K., Harward, M.E., 1974. Amorphous Clay Constituents of Soils, in: Brady, N.C. (Ed.), *Advances in Agronomy*. Academic Press, pp. 211–260. [https://doi.org/10.1016/S0065-2113\(08\)60872-X](https://doi.org/10.1016/S0065-2113(08)60872-X)
- Wagai, R., Mayer, L.M., 2007. Sorptive stabilization of organic matter in soils by hydrous iron oxides. *Geochim. Cosmochim. Acta* 71, 25–35. <https://doi.org/10.1016/j.gca.2006.08.047>
- 535 Wan, J., Tyliszczak, T., Tokunaga, T.K., 2007. Organic carbon distribution, speciation, and elemental correlations within soil microaggregates: Applications of STXM and NEXAFS spectroscopy. *Geochim. Cosmochim. Acta* 71, 5439–5449. <https://doi.org/10.1016/j.gca.2007.07.030>